

Accepted Manuscript

Multitrace/singletrace formulations and Domain Decomposition Methods for the solution of Helmholtz transmission problems for bounded composite scatterers

Carlos Jerez-Hanckes, Carlos Pérez-Arancibia, Catalin Turc

PII: S0021-9991(17)30631-9
DOI: <http://dx.doi.org/10.1016/j.jcp.2017.08.050>
Reference: YJCPH 7552

To appear in: *Journal of Computational Physics*

Received date: 11 January 2017
Revised date: 16 August 2017
Accepted date: 24 August 2017

Please cite this article in press as: C. Jerez-Hanckes et al., Multitrace/singletrace formulations and Domain Decomposition Methods for the solution of Helmholtz transmission problems for bounded composite scatterers, *J. Comput. Phys.* (2017), <http://dx.doi.org/10.1016/j.jcp.2017.08.050>

This is a PDF file of an unedited manuscript that has been accepted for publication. As a service to our customers we are providing this early version of the manuscript. The manuscript will undergo copyediting, typesetting, and review of the resulting proof before it is published in its final form. Please note that during the production process errors may be discovered which could affect the content, and all legal disclaimers that apply to the journal pertain.



Multitrace/singletrace formulations and Domain Decomposition Methods for the solution of Helmholtz transmission problems for bounded composite scatterers

Carlos Jerez-Hanckes, Carlos Pérez-Arancibia, Catalin Turc

Abstract

We present Nyström discretizations of multitrace/singletrace formulations and non-overlapping Domain Decomposition Methods (DDM) for the solution of Helmholtz transmission problems for bounded composite scatterers with piecewise constant material properties. We investigate the performance of DDM with both classical Robin and optimized transmission boundary conditions. The optimized transmission boundary conditions incorporate square root Fourier multiplier approximations of Dirichlet to Neumann operators. While the multitrace/singletrace formulations as well as the DDM that use classical Robin transmission conditions are not particularly well suited for Krylov subspace iterative solutions of high-contrast high-frequency Helmholtz transmission problems, we provide ample numerical evidence that DDM with optimized transmission conditions constitute efficient computational alternatives for these type of applications. In the case of large numbers of subdomains with different material properties, we show that the associated DDM linear system can be efficiently solved via hierarchical Schur complements elimination.

Keywords: multiple junctions, multitrace formulations, single trace formulations, domain decomposition methods.

AMS subject classifications: 65N38, 35J05, 65T40, 65F08

1 Introduction

The phenomenon of electromagnetic wave scattering by bounded penetrable objects composed of several subdomains with different but constant electric permittivities, is relevant for numerous applications in antenna design, diffraction gratings, and photovoltaic cells, to name but a few. It is typical in all these application areas that multiple media meet at a single point, a scenario that is referred to as *triple or multiple junctions*. Standard numerical methods perform poorly when dealing with wave scattering by composite objects with piecewise constant material properties spanning large frequency ranges, as they need to resolve wave interactions with high-contrast sharp interfaces. Volumetric discretizations of these problems result in very large linear systems of equations that are ill-conditioned in the high-frequency regime and whose solution by iterative solvers require inordinate numbers of iterations. Several preconditioning strategies have been proposed to mitigate the aforementioned issues, the most successful arguably being those that rely on the shifted Laplacean [3, 13] or the sweeping preconditioner introduced in [12].

Domain Decomposition Methods (DDM) are natural candidates for the solution of scattering problems involving composite scatterers. DDM are divide and conquer strategies whereby the computational domain is divided into smaller subdomains for which solutions are matched via transmission conditions on subdomain interfaces. The convergence of DDM for time-harmonic

wave scattering applications depends a great deal on the choice of the transmission conditions that allow the exchange of information between adjacent subdomains. These interface transmission conditions should ideally allow information to flow out of a subdomain with as little as possible information being reflected back into the subdomain. Thus, the interface transmission conditions fall into the category of Absorbing Boundary Conditions (ABC). From this perspective, the ideal choice of transmission conditions on an interface between two subdomains is such that the impedance/transmission operator is the restriction to the common interface of the Dirichlet-to-Neumann (DtN) operator corresponding to the adjacent subdomain. Traditionally, the interface transmission conditions were chosen as the classical first order ABC outgoing Robin/impedance boundary conditions [11, 15]. The convergence of DDM with classical Robin interface boundary conditions is slow and is adversely affected by the number of subdomains. Fortunately, the convergence of DDM can be considerably improved through incorporation of ABC that constitute higher order approximations of DtN operators in the form of second order approximations with optimized tangential derivative coefficients [14], square root approximations [4], or other types of non-local transmission conditions [15, 31]. Alternatively, so-called Perfectly Matched Layers can be used at subdomain interfaces [32]. Although the use of more sophisticated ABC, as those recounted above, accelerates a great deal the convergence of DDM, the number of iterations required for convergence still grows –albeit not drastically– with the frequency and number of subdomains. This is not entirely surprising since higher order ABC only involve local exchange of information between adjacent subdomains, and affect to a lesser degree the global exchange of information between distant subdomains. Recent efforts have been devoted to construct “double sweep”-type preconditioners that address the latter issue [34, 35]. The resulting preconditioned DDM scale favorably with frequency and number of subdomains, but appear to be somewhat less effective for wave propagation problems in composite media that exhibit sharp high-contrast interfaces.

Boundary integral equation based solvers for scattering by composite objects with piecewise constant material properties require significantly fewer unknowns than volumetric solvers as only the interfaces of material discontinuity need be discretized. The formulation of these problems in terms of robust boundary integral equations has recently received significant interest in the community, the main achievement being the introduction of Multi-Trace (MTF) and Single-Trace Formulations (STF) [18, 8, 30]. The derivation of the MTF consists of the following steps: (1) use of Green’s identities in each subdomain, whose boundary is a union of interfaces of material discontinuity, to represent the fields in that subdomain via layer potentials; (2) application of Dirichlet and Neumann traces associated to that subdomain to the Green’s identities; followed by (3) enforcement of the continuity conditions across interfaces to replace the identity terms in the previous steps by Dirichlet and Neumann traces of solutions in adjacent subdomains. This procedure leads to a boundary integral equation of the first kind whose unknowns are both interior and exterior Dirichlet and Neumann traces of fields on each interface and which involves the standard Boundary Integral Operators (BIO) on each subdomain corresponding to the wavenumber associated with that subdomain. Galerkin discretizations of the MTF for relative low frequencies preconditioned by diagonal or Calderón preconditioners yield small Krylov subspace iteration numbers [20, 21]. However, as contrast ratios increase, the Calderón preconditioners are less effective when used for low order Galerkin discretizations. The STF, on the other hand, are systems of boundary integral equations that are natural generalizations of the classical Müller formulations [26]: the fields are sought in terms of suitable linear combinations of layer potentials defined on the union of all interfaces—typically referred to as the *skeleton*—of material discontinuity [8, 17, 30] in a manner that gives rise to cancellation of hypersingular operators. On account of being integral equations of the

second kind, STF can be well suited for iterative solvers in certain settings, see the comprehensive reference [30]. We mention that direct solvers based on matrix compression techniques have been proposed in the literature for the efficient solution of STF in the high-frequency, high-contrast regime [17].

In this paper, we compare the performance of Nyström solvers based multitrace/singletrace formulations and DDM solvers in the case of high-frequency scattering problems from composite high-contrast scatterers. A major advantage of MTF/STF is the ease with which existing boundary integral operator discretizations can be incorporated in those formulations. We present in this work a straightforward extension of the Helmholtz transmission Nyström solvers introduced in [?] to MTF/STF. Unlike STF, MTF are readily amenable to analytical preconditioners. We investigate two types of simple preconditioners for MTF: the Calderón preconditioner proposed in [18] and a new preconditioner that combines a Schur complement approach with a Calderón preconditioner. Both preconditioners are shown to be effective for high-frequency high-contrast scattering problems from composite scatterers not depending on the number of subdomains. However, the numbers of iterations required by Nyström discretizations of MTF grows considerably with the frequency and/or the contrast between subdomains, even after resorting to preconditioning. We show that in the aforementioned frequency regime DDM based on boundary integral equations constitute advantageous alternatives to MTF/STF. We investigate both DDM based on the exchange of classical Robin data between subdomain as well as DDM that incorporate general Robin/impedance boundary operators that are square root approximations of DtN maps [19]. In both cases, we solve the subdomain Helmholtz equations with Robin or generalized Robin boundary conditions using well-conditioned boundary integral formulations solved by Nyström discretizations [33]. Provided the size of the subdomains is small enough—in terms of wavelengths across, the latter problems can be solved by direct linear algebra methods.

The numerical results presented in this paper corroborate the well-known fact that DDM based on classical Robin boundary conditions do not perform well as either the frequency or/and the number of subdomains are increased. We present two possible approaches to overcome this shortcoming. The first approach we pursue is to incorporate square root approximations—using complex wavenumbers—of the DtN operators as generalized Robin operators in DDM. The operators were used successfully for regularizing boundary integral equations at high frequencies [2, 1, 6, 5, ?, 7] and also incorporated successfully in DDM [4, 34]. Since for composite scatterers, adjacent subdomains may have different material properties (hence wavenumbers), we blend the approximations of DtN operators corresponding to different subdomains—with different wavenumbers as well—via smooth cutoff functions. The second approach is a direct solver of the DDM linear system based on hierarchical elimination via Schur complements of the Robin data corresponding to interior subdomain interfaces. This idea was presented recently as a hierarchical merging of Robin-to-Robin (RtR) maps [16, 28] in the context of scattering from variable media with smooth index of refraction as well as multiple scattering. The advantage of the Schur complement DDM is that at each stage inverses of relatively small matrices need be computed, and these can be performed in a hierarchical fashion that optimizes the computational cost.

The use of boundary integral equations in a DDM setting allows for larger sized subdomains and efficient treatment of unbounded domains [31]. Further advantages can be garnered from using Nyström discretizations in conjunction with boundary integral equations DDM. Indeed, (a) the square root DtN approximations which are naturally defined in the Fourier domain can be implemented with ease as Fourier multipliers using FFTs and (b) the regularization strategy presented in [33] is applicable to general Robin boundary conditions that involve the square root operators.

In contrast, boundary element discretizations require either local approximations or rational Padé approximations of the square root operators [4, 34]. In addition, neither the presence of cross points at multiple junctions nor the incorporation of square root DtN approximations as generalized Robin boundary conditions affect the accuracy of the DDM solvers. The Nyström DDM with optimized transmission conditions requires much fewer iterations than the DDM with classical Robin transmission conditions, while the computational cost of the local subdomain solves for the former method is virtually the same as that for the latter.

In this contribution we present two-dimensional results. The extension of the DDM based on Nyström discretizations of boundary integral operators to three dimensional configurations faces additional challenges related to surface parametrizations, singular quadratures, and resolution of multiple junction singularities.

The structure of this paper is as follows. Section 2 describes the transmission problem in composite domains; Section 3 reviews both MTF and STF approaches. The DDM approach with all its variants is then introduced in Section 4. Section 5 discusses high-order Nyström discretizations of the MTF/STF, as well as Nyström discretizations of the Robin-to-Robin maps that are central to DDM, while a variety of numerical results are shown in Section 6. Finally, the conclusions of this work are presented in Section 7.

2 Scalar transmission problems in composite domains

We consider the problem of two dimensional electromagnetic scattering by structures that feature multiple junctions, i.e. physical points where at least three interfaces of material discontinuity meet (e.g. the structure displayed in Figure 1). For the sake of presentation simplicity, we focus our treatment of transmission problems with multiple junction domains on the three subdomain case depicted in Figure 1. We thus consider the problem of scattering of a TM-polarized incident field u^{inc} that impinges on the dielectric structure depicted in Figure 1. Letting u_0 denote the z -component (out-of-plane) of the scattered magnetic field in Ω_0 , and u_j the z -component of the total magnetic field in Ω_j for $j = 1, 2$, we seek to solve the following scalar Helmholtz transmission problem:

$$\begin{aligned} \Delta u_j + k_j^2 u_j &= 0 && \text{in } \Omega_j, \\ u_j + \delta_j^0 u^{inc} &= u_\ell + \delta_\ell^0 u^{inc} && \text{on } \Gamma_{j\ell} = \partial\Omega_j \cap \partial\Omega_\ell, \\ \varepsilon_j^{-1}(\partial_{n_j} u_j + \delta_j^0 \partial_{n_j} u^{inc}) &= -\varepsilon_\ell^{-1}(\partial_{n_\ell} u_\ell + \delta_\ell^0 \partial_{n_\ell} u^{inc}) && \text{on } \Gamma_{j\ell}, \\ \lim_{r \rightarrow \infty} r^{1/2}(\partial u_0 / \partial r - ik_0 u_0) &= 0, \end{aligned} \tag{2.1}$$

where δ_j^0 and δ_ℓ^0 stand for Kronecker operators, that is δ_j^0 is the identity operator if $j = 0$ and the null operator otherwise. The wavenumber k_j in the subdomain Ω_j is given by $k_j = \omega\sqrt{\varepsilon_j}$ in terms of the angular frequency $\omega > 0$ and the electric permittivity ε_j . Throughout this paper we assume that all the permittivities ε_j are positive real numbers, extensions to more general cases being straightforward. The unit normal to the boundary $\partial\Omega_j$ is here denoted by n_j and is assumed to point to the exterior of the subdomain Ω_j . The incident field u^{inc} , on the other hand, is assumed to satisfy the Helmholtz equation with wavenumber k_0 in the unbounded domain Ω_0 . Finally, we point out that the well-posedness of the transmission problem (2.1) is discussed in [18] and references therein.

In what follows, we review three main formulations of the transmission problem (2.1). Two

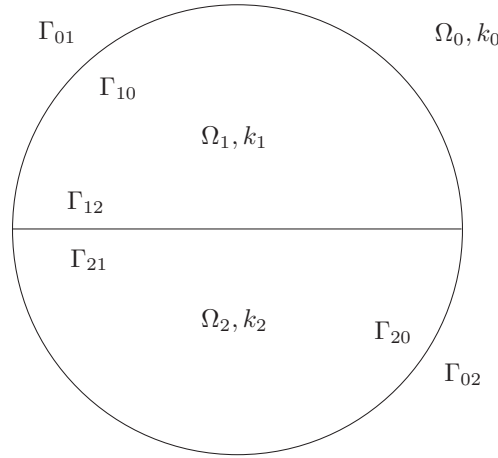


Figure 1: Typical triple junction configuration.

such formulations rely on boundary integral equations, while the third is a domain decomposition method.

3 Multitrace and singletrace formulations

In this section we review the derivation of the MTF [18] and the STF [8] of the transmission problem (2.1). To this end, we make use of the four BIO associated with the Calderón calculus for Lipschitz domains [25]. Let $D \subset \mathbb{R}^2$ be a bounded domain whose boundary $\partial D = \Gamma$ is a closed Lipschitz curve. Given a wavenumber $k > 0$, and a density $\varphi : \Gamma \rightarrow \mathbb{C}$, we recall the definitions of the single layer potential

$$[SL_{\Gamma,k}(\varphi)](\mathbf{z}) := \int_{\Gamma} G_k(\mathbf{z} - \mathbf{y}) \varphi(\mathbf{y}) ds(\mathbf{y}), \quad \mathbf{z} \in \mathbb{R}^2 \setminus \Gamma,$$

and the double layer potential

$$[DL_{\Gamma,k}(\varphi)](\mathbf{z}) := \int_{\Gamma} \frac{\partial G_k(\mathbf{z} - \mathbf{y})}{\partial \mathbf{n}(\mathbf{y})} \varphi(\mathbf{y}) ds(\mathbf{y}), \quad \mathbf{z} \in \mathbb{R}^2 \setminus \Gamma,$$

where $G_k(\mathbf{x}) = \frac{i}{4} H_0^{(1)}(k|\mathbf{x}|)$ denotes the free-space two-dimensional Green's function of the Helmholtz equation with wavenumber k , and \mathbf{n} denotes the unit normal pointing outside the domain D . Applying exterior (resp. interior) Dirichlet and Neumann traces on Γ , which are denoted by $\gamma_{\Gamma}^{D,\text{ext}}$ and $\gamma_{\Gamma}^{N,\text{ext}}$ (resp. $\gamma_{\Gamma}^{D,\text{int}}$ and $\gamma_{\Gamma}^{N,\text{int}}$), respectively, to the single and double layer potentials, we define the four Helmholtz BIO: single layer ($S_{\Gamma,k}$), double layer ($K_{\Gamma,k}$), adjoint double layer ($K_{\Gamma,k}^{\top}$) and hypersingular ($N_{\Gamma,k}$) operators, which satisfy

$$\begin{aligned} \gamma_{\Gamma}^{D,\text{ext}} SL_{\Gamma,k}(\varphi) &= \gamma_{\Gamma}^{D,\text{int}} SL_{\Gamma,k}(\varphi) = S_{\Gamma,k} \varphi, & \gamma_{\Gamma}^{N,\text{ext}} DL_{\Gamma,k}(\varphi) &= \gamma_{\Gamma}^{N,\text{int}} DL_{\Gamma,k}(\varphi) = N_{\Gamma,k} \varphi, \\ \gamma_{\Gamma}^{N,\text{ext}} SL_{\Gamma,k}(\varphi) &= -\frac{\varphi}{2} + K_{\Gamma,k}^{\top} \varphi, & \gamma_{\Gamma}^{D,\text{ext}} DL_{\Gamma,k}(\varphi) &= \frac{\varphi}{2} + K_{\Gamma,k} \varphi, \\ \gamma_{\Gamma}^{N,\text{int}} SL_{\Gamma,k}(\varphi) &= \frac{\varphi}{2} + K_{\Gamma,k}^{\top} \varphi, & \gamma_{\Gamma}^{D,\text{int}} DL_{\Gamma,k}(\varphi) &= -\frac{\varphi}{2} + K_{\Gamma,k} \varphi. \end{aligned} \quad (3.1)$$

In what follows we replace the subindex k in the definition of the layer potentials and BIO by the subindex j of the wavenumber k_j corresponding to the Ω_j subdomain.

3.1 First kind MTF

In this section we derive the first-kind MTF system of integral equations for the transmission problem (2.1). From the Green's representation formula [25] applied to u_j , $j = 0, 1, 2$, we obtain

$$u_j = -DL_{\partial\Omega_j,j}(u_j) + SL_{\partial\Omega_j,j}(\partial_{n_j}u_j) \quad \text{in } \Omega_j. \quad (3.2)$$

Applying the interior Dirichlet trace $\gamma_{\partial\Omega_0}^{D,\text{int}}$ on $\partial\Omega_0$ to the $j = 0$ instance of the identity (3.2) and using the mapping properties (3.1), we get

$$\frac{1}{2}u_0 + K_{\partial\Omega_0,0}(u_0) - \varepsilon_0 S_{\partial\Omega_0,0}(\varepsilon_0^{-1}\partial_{n_0}u_0) = 0 \quad \text{on } \partial\Omega_0. \quad (3.3)$$

The continuity of the total magnetic field across the material interface $\partial\Omega_0$ (cf. (2.1)), that is

$$u_0 = \begin{cases} u_1 - u^{inc} & \text{on } \Gamma_{01}, \\ u_2 - u^{inc} & \text{on } \Gamma_{02}, \end{cases}$$

can be expressed in the equivalent form

$$u_0 = X_{01}u_1 + X_{02}u_2 - u^{inc} \quad \text{on } \partial\Omega_0, \quad (3.4)$$

where the operators X_{01} and X_{02} are defined as

$$X_{01} := E_{01}^{(0)}\Pi_{01} \quad \text{and} \quad X_{02} := E_{02}^{(0)}\Pi_{02},$$

respectively, in terms of the restriction operators Π_{ij} , $\Pi_{ij}\psi := \psi|_{\Gamma_{ij}}$, onto the interface $\Gamma_{ij} = \partial\Omega_i \cap \partial\Omega_j$ for a density function ψ defined on $\partial\Omega_i$ or $\partial\Omega_j$ —in the cases when $i \neq j$ and the domains Ω_i and Ω_j share an edge—and the extension-by-zero operators defined as

$$E_{01}^{(0)}\psi_{01} := \begin{cases} \psi_{01}, & \text{on } \Gamma_{01}, \\ 0, & \text{on } \Gamma_{02}, \end{cases} \quad \text{and} \quad E_{02}^{(0)}\psi_{02} := \begin{cases} 0, & \text{on } \Gamma_{01}, \\ \psi_{02}, & \text{on } \Gamma_{02}, \end{cases}$$

for two functions ψ_{01} and ψ_{02} defined on Γ_{01} and Γ_{02} , respectively. Using the reformulation (3.4) we can re-express equation (3.3) in the following form

$$K_{\partial\Omega_0,0}(u_0) - \varepsilon_0 S_{\partial\Omega_0,0}(\varepsilon_0^{-1}\partial_{n_0}u_0) + \frac{1}{2}X_{01}u_1 + \frac{1}{2}X_{02}u_2 = \frac{1}{2}u^{inc} \quad \text{on } \partial\Omega_0. \quad (3.5)$$

Remark 3.1 *The expressions u_1 and u_2 in equation (3.5) should be understood as Dirichlet traces $u_1|_{\partial\Omega_1}$ and $u_2|_{\partial\Omega_2}$. We prefer the simpler notation as the meaning of those expressions should be grasped from the domain of definition of the operators that act upon them. Furthermore, all the restriction/extension operators can be defined for distributions [18].*

Similarly, applying the interior Neumann trace $\gamma_{\partial\Omega_0}^{N,\text{int}}$ on $\partial\Omega_0$ to the the $j = 0$ instance of representation formula (3.2), we obtain

$$\frac{1}{2}\varepsilon_0^{-1}\partial_{n_0}u_0 - K_{\partial\Omega_0,0}^\top(\varepsilon_0^{-1}\partial_{n_0}u_0) + \varepsilon_0^{-1}N_{\partial\Omega_0,0}(u_0) = 0 \quad \text{on } \partial\Omega_0. \quad (3.6)$$

The continuity condition on $\partial\Omega_0$ of the total tangential electric field (cf. (2.1)), that is

$$\varepsilon_0^{-1}\partial_{n_0}u_0 := \begin{cases} -\varepsilon_1^{-1}\partial_{n_1}u_1 - \varepsilon_0^{-1}\partial_{n_0}u^{inc} & \text{on } \Gamma_{01}, \\ -\varepsilon_2^{-1}\partial_{n_2}u_2 - \varepsilon_0^{-1}\partial_{n_0}u^{inc} & \text{on } \Gamma_{02}, \end{cases}$$

can be expressed in the equivalent form

$$\varepsilon_0^{-1} \partial_{n_0} u_0 = -X_{01}(\varepsilon_1^{-1} \partial_{n_1} u_1) - X_{02}(\varepsilon_2^{-1} \partial_{n_2} u_2) - \varepsilon_0^{-1} \partial_{n_0} u^{inc} \quad \text{on } \partial\Omega_0, \quad (3.7)$$

and thus, equation (3.6) can be expressed as

$$\varepsilon_0^{-1} N_{\partial\Omega_0,0}(u_0) - K_{\partial\Omega_0,0}^\top(\varepsilon_0^{-1} \partial_{n_0} u_0) - \frac{1}{2} X_{01}(\varepsilon_1^{-1} \partial_{n_1} u_1) - \frac{1}{2} X_{02}(\varepsilon_2^{-1} \partial_{n_2} u_2) = \frac{1}{2} \varepsilon_0^{-1} \partial_{n_0} u^{inc} \quad \text{on } \partial\Omega_0. \quad (3.8)$$

We now introduce the Calderón block operators

$$\mathcal{C}_j := \begin{bmatrix} K_{\partial\Omega_j,j} & -\varepsilon_j S_{\partial\Omega_j,j} \\ \varepsilon_j^{-1} N_{\partial\Omega_j,j} & -K_{\partial\Omega_j,j}^\top \end{bmatrix}, \quad j = 0, 1, 2,$$

which satisfy

$$\mathcal{C}_j^2 = \frac{1}{4} \begin{bmatrix} I & 0 \\ 0 & I \end{bmatrix}, \quad (3.9)$$

and also introduce the following matrix operators:

$$\mathbb{X}_{01} = \begin{bmatrix} X_{01} & 0 \\ 0 & -X_{01} \end{bmatrix} \quad \text{and} \quad \mathbb{X}_{02} = \begin{bmatrix} X_{02} & 0 \\ 0 & -X_{02} \end{bmatrix}. \quad (3.10)$$

Denoting the Cauchy data on $\partial\Omega_j$ by

$$\mathbf{u}_j := \begin{bmatrix} u_j \\ \varepsilon_j^{-1} \partial_{n_j} u_j \end{bmatrix}, \quad j = 0, 1, 2,$$

and the incident data \mathbf{u}^{inc} on $\partial\Omega_0$ by

$$\mathbf{u}^{inc} := \begin{bmatrix} u^{inc} \\ \varepsilon_0^{-1} \partial_{n_0} u^{inc} \end{bmatrix},$$

we can re-write equations (3.5) and (3.8) in the form

$$\mathcal{C}_0 \mathbf{u}_0 + \frac{1}{2} \mathbb{X}_{01} \mathbf{u}_1 + \frac{1}{2} \mathbb{X}_{02} \mathbf{u}_2 = \frac{1}{2} \mathbf{u}^{inc} \quad \text{on } \partial\Omega_0. \quad (3.11)$$

Similar techniques applied to u_1 in the domain Ω_1 and respectively u_2 in the domain Ω_2 lead to two additional equations in the vein of equation (3.11) leading to the local MTF [18]:

$$\begin{bmatrix} \mathcal{C}_0 & \mathbb{X}_{01} & \mathbb{X}_{02} \\ \mathbb{X}_{10} & \mathcal{C}_1 & \mathbb{X}_{12} \\ \mathbb{X}_{20} & \mathbb{X}_{21} & \mathcal{C}_2 \end{bmatrix} \begin{bmatrix} \mathbf{u}_0 \\ \mathbf{u}_1 \\ \mathbf{u}_2 \end{bmatrix} = \frac{1}{2} \begin{bmatrix} \mathbf{u}^{inc} \\ -\mathbb{X}_{10} \mathbf{u}^{inc} \\ -\mathbb{X}_{20} \mathbf{u}^{inc} \end{bmatrix}, \quad (3.12)$$

where the additional matrix operators $\mathbb{X}_{j\ell}$ in (3.12) are defined as the operators \mathbb{X}_{01} and \mathbb{X}_{02} in (3.10), but in terms of restriction and extension-by-zero operators $\Pi_{j\ell}$ and $X_{j\ell}$, respectively.

The well-posedness of the local MTF (3.12) in the multitrace space $\prod_{j=0}^2 (H^{1/2}(\partial\Omega_j) \times H^{-1/2}(\partial\Omega_j))$ was established in reference [18]. We note that owing to the presence of both weakly singular and hypersingular operators in the Calderón block operators $\mathcal{C}_j, j = 0, 1, 2$, MTF (3.12) are boundary integral equations of the first kind. As such, the number of iterations needed by Krylov subspace

iterative solvers (e.g. GMRES) to solve the discretized versions of (3.12) can be significant, especially for high-contrast configurations at high-frequencies. Fortunately, simple and quite effective preconditioners for (3.12) are readily available. Indeed, in view of the identity (3.9), a simple preconditioner is the Calderón diagonal preconditioner [18] that turns (3.12) into

$$\begin{bmatrix} \mathcal{C}_0 & 0 & 0 \\ 0 & \mathcal{C}_1 & 0 \\ 0 & 0 & \mathcal{C}_2 \end{bmatrix} \begin{bmatrix} \mathbb{X}_{01} & \mathbb{X}_{02} \\ \mathbb{X}_{10} & \mathbb{X}_{12} \\ \mathbb{X}_{20} & \mathbb{X}_{21} \end{bmatrix} \begin{bmatrix} \mathbf{u}_0 \\ \mathbf{u}_1 \\ \mathbf{u}_2 \end{bmatrix} = \frac{1}{2} \begin{bmatrix} \mathcal{C}_0 & 0 & 0 \\ 0 & \mathcal{C}_1 & 0 \\ 0 & 0 & \mathcal{C}_3 \end{bmatrix} \begin{bmatrix} \mathbf{u}^{inc} \\ -\mathbb{X}_{10}\mathbf{u}^{inc} \\ -\mathbb{X}_{20}\mathbf{u}^{inc} \end{bmatrix}, \quad (3.13)$$

which is a second-kind system of integral equations whose discretized version can be solved in few iterations of a Krylov subspace linear algebra solver.

Another possibility is to eliminate the unknown \mathbf{u}_0 from the MTF (3.12) using Schur complements. Indeed, using the fact that \mathcal{C}_0 is a projector, we get that \mathbf{u}_0 can be explicitly eliminated from the MTF system (3.12) via the equation

$$\mathbf{u}_0 = 2\mathcal{C}_0\mathbf{u}^{inc} - 4\mathcal{C}_0\mathbb{X}_{01}\mathbf{u}_1 - 4\mathcal{C}_0\mathbb{X}_{02}\mathbf{u}_2,$$

leading to a reduced MTF:

$$\begin{bmatrix} \mathcal{C}_1 - 4\mathbb{X}_{10}\mathcal{C}_0\mathbb{X}_{01} & \mathbb{X}_{12} - 4\mathbb{X}_{10}\mathcal{C}_0\mathbb{X}_{02} \\ \mathbb{X}_{21} - 4\mathbb{X}_{20}\mathcal{C}_0\mathbb{X}_{01} & \mathcal{C}_2 - 4\mathbb{X}_{20}\mathcal{C}_0\mathbb{X}_{02} \end{bmatrix} \begin{bmatrix} \mathbf{u}_1 \\ \mathbf{u}_2 \end{bmatrix} = -\frac{1}{2} \begin{bmatrix} \mathbb{X}_{10}\mathbf{u}^{inc} \\ \mathbb{X}_{20}\mathbf{u}^{inc} \end{bmatrix} - 2 \begin{bmatrix} \mathbb{X}_{10}\mathcal{C}_0\mathbf{u}^{inc} \\ \mathbb{X}_{20}\mathcal{C}_0\mathbf{u}^{inc} \end{bmatrix}. \quad (3.14)$$

Formulation (3.14), in turn, can be further preconditioned by the operator $\text{diag}(\mathcal{C}_1, \mathcal{C}_2)$, leading to the following Calderón preconditioned reduced MTF:

$$\begin{bmatrix} \mathcal{C}_1 & 0 \\ 0 & \mathcal{C}_2 \end{bmatrix} \begin{bmatrix} \mathcal{C}_1 - 4\mathbb{X}_{10}\mathcal{C}_0\mathbb{X}_{01} & \mathbb{X}_{12} - 4\mathbb{X}_{10}\mathcal{C}_0\mathbb{X}_{02} \\ \mathbb{X}_{21} - 4\mathbb{X}_{20}\mathcal{C}_0\mathbb{X}_{01} & \mathcal{C}_2 - 4\mathbb{X}_{20}\mathcal{C}_0\mathbb{X}_{02} \end{bmatrix} \begin{bmatrix} \mathbf{u}_1 \\ \mathbf{u}_2 \end{bmatrix} = -\frac{1}{2} \begin{bmatrix} \mathcal{C}_1\mathbb{X}_{10}\mathbf{u}^{inc} \\ \mathcal{C}_2\mathbb{X}_{20}\mathbf{u}^{inc} \end{bmatrix} - 2 \begin{bmatrix} \mathcal{C}_1\mathbb{X}_{10}\mathcal{C}_0\mathbf{u}^{inc} \\ \mathcal{C}_2\mathbb{X}_{20}\mathcal{C}_0\mathbf{u}^{inc} \end{bmatrix}. \quad (3.15)$$

We note that both preconditioned MTF (3.13) and (3.15) do not require significant computational overhead with respect to the original MTF (3.12).

3.2 Second kind STF

An alternative boundary integral equation formulation of the transmission problem (2.1) can be derived using layer potentials defined on the skeleton $\Gamma := \Gamma_{01} \cup \Gamma_{12} \cup \Gamma_{02}$ whose segments are oriented clockwise [8]. In this approach, the solutions $u_j, j = 0, 1, 2$ of the transmission problem (2.1) are sought in the form

$$u_j(\mathbf{x}) := SL_{\Gamma,j} v - \varepsilon_j DL_{\Gamma,j} p, \quad \mathbf{x} \in \Omega_j, \quad (3.16)$$

where v and p are densities defined on the skeleton Γ and the double layer operators are defined with respect to exterior unit normals \mathbf{n} with respect to the orientation chosen on Γ . Here we used the same convention that the index j in equation (3.16) refers to the wavenumber k_j for $j = 0, 1, 2$. The enforcement of the transmission conditions on the interfaces between subdomains leads to the following system of boundary integral equations, for all $\ell, j = 0, 1, 2$ such that $\ell < j$:

$$\begin{aligned} \frac{\varepsilon_\ell + \varepsilon_j}{2} p + (-1)^\ell [S_\ell - S_j] v + (-1)^\ell [\varepsilon_\ell K_\ell - \varepsilon_j K_j] p &= \begin{cases} -u^{inc} & \text{if } \ell = 0 \\ 0 & \text{otherwise} \end{cases} \quad \text{on } \Gamma_{\ell j}, \\ \frac{\varepsilon_\ell^{-1} + \varepsilon_j^{-1}}{2} v + (-1)^\ell [\varepsilon_j^{-1} S_j - \varepsilon_\ell^{-1} S_\ell] v + (-1)^\ell [N_j - N_\ell] p &= \begin{cases} -\varepsilon_0^{-1} \partial_n u^{inc} & \text{if } \ell = 0 \\ 0 & \text{otherwise} \end{cases} \quad \text{on } \Gamma_{\ell j}. \end{aligned} \quad (3.17)$$

In what follows we refer to the formulation (3.17) by the acronym STF. All of the boundary integral operators featured in equation (3.17) are defined on the skeleton Γ . The presence of (a) multiples of the densities v and p as well as (b) differences of hypersingular operators $N_j - N_\ell$ suggest referring to equations (3.17) as second kind boundary integral equations. We note that in contrast to the MTF (3.12), the second kind equations (3.17) require two (scalar) unknowns per interface $\Gamma_{j\ell}$. To the best of our knowledge, the well-posedness of second kind boundary integral equations (3.17) is still an open question; see the discussion on this in [9]. Our numerical experiments indicate that these formulations appears to be well posed for a wide range of wavenumbers $k_j, j = 0, 1, 2$, thus corroborating the findings in [9].

4 Domain decomposition approach with classical Robin boundary conditions

DDM are natural candidates for numerical solution of transmission problems (2.1). A non-overlapping domain decomposition approach for the solution of equations (2.1) consists of solving subdomain problems with matching Robin boundary conditions on the common subdomain interfaces [11]. Indeed, this procedure amounts to computing the subdomain solutions:

$$\begin{aligned} \Delta u_j + k_j^2 u_j &= 0 & \text{in } \Omega_j, \\ \Delta u_\ell + k_\ell^2 u_\ell &= 0 & \text{in } \Omega_\ell, \\ \varepsilon_j^{-1}(\partial_{n_j} u_j + \delta_j^0 \partial_{n_j} u^{inc}) + i\eta(u_j + \delta_j^0 u^{inc}) &= -\varepsilon_\ell^{-1}(\partial_{n_\ell} u_\ell + \delta_\ell^0 \partial_{n_\ell} u^{inc}) + i\eta(u_\ell + \delta_\ell^0 u^{inc}) & \text{on } \Gamma_{j\ell} \\ \varepsilon_\ell^{-1}(\partial_{n_\ell} u_\ell + \delta_\ell^0 \partial_{n_\ell} u^{inc}) + i\eta(u_\ell + \delta_\ell^0 u^{inc}) &= -\varepsilon_j^{-1}(\partial_{n_j} u_j + \delta_j^0 \partial_{n_j} u^{inc}) + i\eta(u_j + \delta_j^0 u^{inc}) & \text{on } \Gamma_{\ell j}. \end{aligned} \quad (4.1)$$

In equations (4.1), η is assumed to be a positive number. The latter requirement is needed to ensure the well-posedness of the impedance boundary value Helmholtz problem in the exterior domain Ω_0 [10].¹

In order to describe the DDM method more concisely we introduce subdomain Robin-to-Robin (RtR) maps [15]. Given a subdomain Ω_j we define the RtR map \mathcal{S}^j in the following manner:

$$\mathcal{S}^j(\psi_j) := (\varepsilon_j^{-1} \partial_{n_j} u_j - i\eta u_j)|_{\partial\Omega_j}, \quad j = 0, 1, 2, \quad (4.2)$$

where u_j is the solution of the following problem:

$$\begin{aligned} \Delta u_j + k_j^2 u_j &= 0 & \text{in } \Omega_j, \\ \varepsilon_j^{-1} \partial_{n_j} u_j + i\eta u_j &= \psi_j & \text{on } \partial\Omega_j. \end{aligned}$$

In the case when Ω_j is the exterior domain Ω_0 , we further require in the definition of the RtR map \mathcal{S}^0 that u_0 is radiative at infinity. The DDM method computes the global Robin data $f = [f_1 \ f_2 \ f_0]^\top$ —the reader should observe the coordinate order—with

$$f_j := (\varepsilon_j^{-1} \partial_{n_j} u_j + i\eta u_j)|_{\partial\Omega_j}, \quad j = 0, 1, 2,$$

as the solution of the following linear system that incorporates the subdomain RtR maps $\mathcal{S}^j, j = 0, 1, 2$, previously defined

$$(I + A)f = g, \quad A := XS, \quad \mathcal{S} := \begin{bmatrix} \mathcal{S}^1 & 0 & 0 \\ 0 & \mathcal{S}^2 & 0 \\ 0 & 0 & \mathcal{S}^0 \end{bmatrix}, \quad X := \begin{bmatrix} 0 & X_{12} & X_{10} \\ X_{21} & 0 & X_{20} \\ X_{01} & X_{02} & 0 \end{bmatrix}. \quad (4.3)$$

¹In all the numerical examples in Section 6 we took $\eta = k_0$.

with right-hand side $g = [g_1 \ g_2 \ g_0]^\top$ wherein

$$\begin{aligned} g_1 &= X_{01}(-\varepsilon_0^{-1}\partial_{n_0}u^{inc} + i\eta u^{inc})|_{\partial\Omega_0}, \\ g_2 &= X_{02}(-\varepsilon_0^{-1}\partial_{n_0}u^{inc} + i\eta u^{inc})|_{\partial\Omega_0}, \\ g_0 &= (-\varepsilon_0^{-1}\partial_{n_0}u^{inc} - i\eta u^{inc})|_{\partial\Omega_0}. \end{aligned}$$

We note that the matrix A in equation (4.3) is not stored in practice, and, due to its possibly large size, the DDM linear system (4.3) is typically solved in practice via iterative methods. Iterative solvers (e.g. Jacobi, GMRES) for the solution of DDM linear systems of the type described in equation (4.3) require large numbers of iterations, especially in the case of larger numbers of subdomains (e.g. see Figure 3 in Section 6). This shortcoming can be attributed to the choice of classical Robin boundary conditions and the outflow/inflow of information from a subdomain to its neighboring subdomains associated with it. Ideally, the subdomain boundary conditions have to be chosen so that information flows out of the subdomain and no information is reflected back into the subdomain. This can be achieved if the multiplicative term $i\eta$ in equations (4.3) is replaced by the adjacent subdomain Dirichlet-to-Neumann (DtN) operator restricted to the common interface—in this way the Jacobi scheme converges in precisely two iterations [27, 19]. Since DtN maps are not always well defined and expensive to calculate even when properly defined, easily computable approximations of DtN maps can be employed effectively to lead to faster convergence rates of GMRES solvers for DDM algorithms [4]. We present in Section 4.1 a non-overlapping DDM based on square root approximations of DtN operators.

4.1 DDM with optimized transmission boundary conditions

The rate of convergence of iterative Krylov subspace solvers of the DDM linear system (4.3) is largely determined by the choice of transmission boundary conditions therein. More effective transmission boundary conditions on the subdomain interfaces are known to improve the performance of iterative DDM solvers [31, 4, 34, 14]. For instance, the ideal transmission operator on the interface Γ_{12} corresponding to the domain Ω_1 consists of the operator $\varepsilon_2^{-1}Y^2|_{\Gamma_{21}}$, where Y^2 is the DtN operator corresponding to the domain Ω_2 with zero Dirichlet boundary conditions on $\partial\Omega_2 \setminus \Gamma_{21}$. With this very choice, the ensuing DDM algorithm converges in precisely two iterations [27], at least in the case when Ω_j are half planes. Similarly, the optimal transmission operator on the interface Γ_{10} corresponding to the domain Ω_1 can be shown to consist of the operator $\varepsilon_0^{-1}Y^0|_{\Gamma_{01}}$. Although DtN operators are not properly defined for interior subdomains for all wavenumbers, they are always well defined in the exterior domain Ω_0 . However, even when they properly defined, DtN maps are non-local operators whose computation can be expensive. Whenever possible, DtN operators can be expressed via boundary integral operators. For instance, using Green's identities in the domain Ω_2 and taking into consideration the null Dirichlet boundary conditions on $\partial\Omega_2 \setminus \Gamma_{21}$, we obtain the expression:

$$u_2 = -DL_{\Gamma_{21},2}(u_2) + SL_{\partial\Omega_2,2}(\partial_{n_2}u_2) \quad \text{in } \Omega_2,$$

which upon application of Dirichlet traces, leads to the identity

$$Y^2 = S_{\partial\Omega_2,2}^{-1} \left(\frac{1}{2}I + K_{\Gamma_{21},2} \right). \quad (4.4)$$

The invertibility of the operator $S_{\partial\Omega_2,2}$ in the equation above, and hence the well-posedness of the DtN operator Y^2 , can be guaranteed provided the subdomain Ω_2 is small enough, typically less

than one wavelength across. A simple solution that would allow one to consider subdomains of any size is to consider DtN operators $Y^{2,c}$ corresponding to complexified wavenumbers $k_2 + i\sigma_2$, $\sigma_2 > 0$ instead of the operators Y^2 . Using these operators, we can define a transmission operator on the interface $\partial\Omega_2$ in the form

$$\mathcal{T}_1^{DtN} = \varepsilon_2^{-1} X_{12} Y^{2,c} + \varepsilon_0^{-1} X_{10} Y^0 \quad (4.5)$$

and similar transmission operators on the interfaces $\partial\Omega_2$ and $\partial\Omega_0$ respectively. We then match DtN Robin boundary conditions on the subdomain interfaces in the form

$$\varepsilon_1^{-1} \partial_{n_1} u_1 + \mathcal{T}_1^{DtN} u_1 = -\varepsilon_j^{-1} (\partial_{n_j} u_j + \delta_j^0 \partial_{n_j} u^{inc}) + \mathcal{T}_1^{DtN} (u_j + \delta_j^0 u^{inc}), \quad j \in \{0, 2\} \quad (4.6)$$

and we refer to the ensuing DDM with transmission conditions defined in equation (4.6) as DDM DtNR.

We reiterate that the DtN operators in (4.6) for the domains Ω_j , $0 \leq j$, even when properly defined, are expensive to compute and to apply. We therefore rely on suitable approximations of DtN operators that can be computed inexpensively and, at the same time, lead to well posed generalized Robin boundary conditions of the form (4.6) on the boundary of the domains Ω_j , $0 \leq j$. These approximations start from an alternative representation of the DtN operators in each domain. For instance, an application of the Neumann trace $\gamma_{\partial\Omega_2}^{N, \text{ext}}$ to the Green's identity

$$u_2 = -DL_{\partial\Omega_2, 2}(u_2) + SL_{\Gamma_{21}, 2}(Y^2 u_2) \quad \text{in } \Omega_2,$$

which assumed $\partial_{n_2} u_2 = Y^2 u_2 = 0$ on $\partial\Omega_2 \setminus \Gamma_{21}$, leads to

$$\left(\frac{1}{2} I - K_{\Gamma_{21}, 2}^\top \right) Y^2 = -N_{\partial\Omega_2, 2},$$

and thus, whenever admissible,

$$Y^2 = - \left(\frac{1}{2} I - K_{\Gamma_{21}, 2}^\top \right)^{-1} N_{\partial\Omega_2, 2}.$$

An explicit approximation of the DtN operator Y^2 can be achieved by keeping the leading order term in the equation above in the sense of pseudodifferential operators

$$Y^2 \approx -2N_{\partial\Omega_2, 2}. \quad (4.7)$$

The restriction of the operators $N_{\partial\Omega_2, 2}$ to the interface Γ_{12} —which is an open arc—has to be performed with care [31, 33]. In addition, the generalized Robin operators should lead to well-posed problems in the domain Ω_1 .

One possibility to blend approximations to $Y^2|_{\Gamma_{21}}$ and $Y^0|_{\Gamma_{20}}$ of the form (4.7) in terms of hypersingular operators is given by [33]:

$$\mathcal{T}_1 = -2\varepsilon_0^{-1} \chi_{01} N_{\partial\Omega_1, k_0 + i\sigma_0} \chi_{01} - 2\varepsilon_2^{-1} \chi_{12} N_{\partial\Omega_1, k_2 + i\sigma_2} \chi_{12}, \quad \sigma_j > 0, \quad (4.8)$$

where χ_{01} and χ_{12} are smooth cutoff functions whose supports lie in Γ_{10} and Γ_{12} , respectively.

Given that the hypersingular operators are relatively expensive to compute, we proceed to replace the hypersingular operators in equation (4.8) by principal symbol Fourier multiplier operators. The latter principal symbols are defined as

$$p^N(\xi, k_0 + i\sigma_0) = -\frac{1}{2} \sqrt{|\xi|^2 - (k_0 + i\sigma_0)^2} \quad \text{and} \quad p^N(\xi, k_2 + i\sigma_2) = -\frac{1}{2} \sqrt{|\xi|^2 - (k_2 + i\sigma_2)^2},$$

where the square root branches are chosen such that the imaginary parts of the principal symbols are positive. The principal symbol Fourier multipliers are defined in the Fourier space $TM(\partial\Omega_1)$ [1] as

$$[PS(N_{\partial\Omega_1, k_j + i\sigma_j})\varphi_1]^\wedge(\xi) = p^N(\xi, k_j + i\sigma_j)\hat{\varphi}_1(\xi) \quad (4.9)$$

for a density φ_1 defined on $\partial\Omega_1$. We define accordingly

$$PS(\mathcal{T}_1) = -2\varepsilon_0^{-1}\chi_{01}PS(N_{\partial\Omega_1, k_0 + i\sigma_0})\chi_{01} - 2\varepsilon_2^{-1}\chi_{12}PS(N_{\partial\Omega_1 k_2 + i\sigma_2})\chi_{12}, \quad \sigma_j > 0, \quad (4.10)$$

and we use the operators in equation (4.10) as transmission operators in the DDM formulation. Thus, the classical Robin boundary conditions on $\partial\Omega_1$ are replaced by the following Generalized Square Root Robin boundary conditions (GSqR)

$$\varepsilon_1^{-1}\partial_{n_1}u_1 + PS(\mathcal{T}_1)u_1 = -\varepsilon_j^{-1}(\partial_{n_j}u_j + \delta_j^0\partial_{n_j}u^{inc}) + PS(\mathcal{T}_1)(u_j + \delta_j^0u^{inc}), \quad j \in \{0, 2\}. \quad (4.11)$$

We note that the operators $PS(\mathcal{T}_1) : H^{1/2}(\partial\Omega_1) \rightarrow H^{-1/2}(\partial\Omega_1)$ are coercive, and thus the Helmholtz equations in the domain Ω_1 with generalized Robin boundary conditions defined by the operators in the left-hand side of equation (4.11) are well posed [33]. Similar generalized impedance operators can be defined for the domains Ω_0 and Ω_2 and then incorporated in a DDM algorithm that computes the generalized Robin data

$$f_j^g := (\varepsilon_j^{-1}\partial_{n_j}u_j + PS(\mathcal{T}_j)u_j)|_{\partial\Omega_j}, \quad 0 \leq j$$

by making use of suitably defined generalized RtR maps; we refer to the ensuing DDM with transmission conditions (4.11) as DDM GSqR.

5 High-order Nyström discretizations

In what follows we use Nyström discretizations of the MTF equation (3.12), STF equation (3.17), as well as the RtR maps associated with the DDM formulation (4.3), the DDM DtNR formulation (4.6), and the DDM GSqR formulation (4.11). The key ingredient is the Nyström discretization of the four BIO in the Calderón calculus for piecewise smooth boundaries. These discretizations were introduced in [?] where this methodology was presented in full detail.

Each subdomain boundary $\partial\Omega_j$ is assumed to be a piece-wise smooth closed curve. Graded meshes produced by means sigmoid transforms [22] that accumulate points polynomially toward the corner and multiple junction points on $\partial\Omega_j$ are utilized. For each of the subdomains Ω_j , $j = 0, 1, 2$, we thus obtain graded meshes denoted by

$$L_j := \{\mathbf{x}_m^j, m = 0, \dots, N_j - 1\} \quad \text{on} \quad \partial\Omega_j,$$

with the same polynomial degree of the sigmoid transforms on all subdomains. All meshes in the parameter space $[0, 2\pi]$ are shifted by the same amount so that none of the grid points on the skeleton corresponds to a triple/multiple junction or a corner point. Using graded meshes that avoid corner points and classical singular quadratures of Kusmaul and Martensen [23, 24], we employ the Nyström discretization presented in [?] to produce high-order $N_j \times N_j$ collocation matrix approximations of the four BIOs in (3.1). In what follows we present specific details on how to use the Nyström discretization of the BIOs to produce discretizations of the various formulations (MTF, STF, and DDM) considered in this text.

Nyström discretization of the MTF equation (3.12). Following the prescriptions in [?] for the discretization of transmission boundary integral equations for one subdomain, i.e. no triple/multiple junctions, we define *weighted* Neumann traces on the boundary of each subdomain Ω_j

$$\partial_{n_j}^w u_j := |\mathbf{x}'_j| \partial_{n_j} u_j \quad (5.1)$$

where \mathbf{x}_j is a $[0, 2\pi]$ parametrization of the boundary $\partial\Omega_j$ that incorporates sigmoid transforms on each of the smooth arcs of $\partial\Omega_j$. The role of the weighted traces (5.1) is to allow for recasting of the integral equation system (3.12) in terms of new unknowns with increased regularity, which, in turn, can be tuned by simply increasing the polynomial order in the sigmoid transforms. This procedure requires introducing *weighted* parametrized versions of the four BIO of the Calderón calculus; these were discussed in detail in the same reference [?].

We note that on a common interface $\Gamma_{j\ell}$ between two subdomains Ω_j and Ω_ℓ that share an edge, the grid points corresponding to the mesh in each subdomain coincide. Owing to this fact, the discretization of the various projection/extension operators in the definition of the $X_{j\ell}$ is straightforward, as it amounts to multiplication by matrices made up of zero and identity blocks.

The discretization of the Calderón operator preconditioning of the MTF via equations (3.13) and (3.15), on the other hand, is effected by multiplication of the collocation matrices corresponding to each BIO featured in those equations. The end result of the Nyström discretization of MTF is the calculation of the Dirichlet and weighted Neumann traces on the global grid $\bigcup_j L_j$ on the skeleton Γ , from which all the physical quantities of interest can be further retrieved from Green's identities (3.2).

Nyström discretization of the STF equation (3.17). The additional challenge in the Nyström discretization of the STF consists of the fact that in the presence of multiple junctions the skeleton Γ cannot be represented via a piece-wise smooth periodic parametrization—recall that the Nyström discretizations that rely on the singular quadratures of Kusmaul and Martensen [23, 24] require that the domain of integration is a closed curve and thus all the integrands to be dealt with are *periodic*. Nevertheless, letting

$$v^w := |\mathbf{x}'|v \quad p^w := |\mathbf{x}'|p \quad \text{on } \Gamma = \Gamma_{01} \cup \Gamma_{12} \cup \Gamma_{02},$$

and multiplying both sides of equations (3.17) by the weight $|\mathbf{x}'|$, we obtain a *weighted* STF whose unknowns are (v^w, p^w) .

We note that the weighted unknowns (v^w, p^w) vanish algebraically at the triple/multiple junction points of the skeleton Γ . This simple fact allows us to evaluate easily weighted boundary integral operators defined on Γ . Indeed, the evaluation of a parametrized weighted integral operator of the type

$$(Iv^w)(\mathbf{x}(t)) = \int_{\Gamma} \mathcal{G}_k^w(\mathbf{x}(t), \mathbf{x}(\tau)) v^w(\mathbf{x}(\tau)) d\tau, \quad \mathbf{x}(t) \in \Gamma_{01},$$

can be simply performed as

$$(Iv^w)(\mathbf{x}(t)) = \int_{\partial\Omega_1} \mathcal{G}_k^w(\mathbf{x}(t), \mathbf{x}(\tau)) v_1^w(\mathbf{x}(\tau)) d\tau + \int_{\partial\Omega_0} \mathcal{G}_k^w(\mathbf{x}(t), \mathbf{x}(\tau)) v_0^w(\mathbf{x}(\tau)) d\tau, \quad (5.2)$$

where

$$v_1^w(\mathbf{x}(\tau)) := v^w(\mathbf{x}(\tau)), \quad \mathbf{x}(\tau) \in \partial\Omega_1 = \Gamma_{01} \cup \Gamma_{12} \quad v_0^w(\mathbf{x}(\tau)) := \begin{cases} v^w(\mathbf{x}(\tau)), & \mathbf{x}(\tau) \in \Gamma_{02} \\ 0, & \mathbf{x}(\tau) \in \Gamma_{02} \end{cases}.$$

Each of the two integrals in equation (5.2) is performed on a closed curve and involves 2π periodic and regular functions, and thus can be computed with high-order accuracy by the Nyström method presented in [?]. All of the weighted integral operators that enter the weighted STF can be effected in a similar manner. We note that the difference of hypersingular operators that features in STF can be performed without recourse to numerical differentiation [?].

Discretization of the various DDM based on Nyström discretizations of the RtR maps. Our DDM discretizations compute approximations of each subdomain Robin data $f_j = (\varepsilon_j^{-1} |\mathbf{x}'_j| \partial_{n_j} u_j + ik_0 u_j)$ collocated at the boundary points L_j . For each subdomain Ω_j we denote the collocated Robin data by the vector $f_j^{N_j}$ of size N_j ; we denote by f^N the vector of global collocated Robin data on the global grid $\bigcup_j L_j$ on the skeleton Γ , that is $f^N = [f_0^{N_0} f_1^{N_1} \dots]^\top$. The global Robin data unknown f^N is computed via Krylov subspace iterative solutions (e.g. GMRES) of the collocation discretization of the DDM linear system (4.3). To this end, each of the RtR maps \mathcal{S}^j that appear in equation (4.3) can be approximated by Nyström collocation matrices at the grid points L_j via well-conditioned BIO and subsequently discretized following the Nyström discretizations introduced in [33]. In a nutshell, the method introduced in [33] is a direct regularized boundary integral equation formulation of interior/exterior Helmholtz equations with Robin/impedance boundary conditions of the type employed by the DDM formulation (4.3). Specifically, if u_j is the solution of the following Helmholtz problem with Robin boundary conditions, augmented by u_0 is radiative in the exterior domain Ω_0 ,

$$\begin{aligned} \Delta u_j + k_j^2 u_j &= 0 \quad \text{in } \Omega_j \\ \varepsilon_j^{-1} \partial_{n_j} u_j + i\eta u_j &= \psi_j \quad \text{on } \partial\Omega_j, \end{aligned}$$

then $u_j|_{\partial\Omega_j}$ can be shown to satisfy the following well-conditioned regularized boundary integral equation [33]:

$$\begin{aligned} \mathcal{A}_j(u_j|_{\partial\Omega_j}) &= \varepsilon_j(S_j + S_{\kappa_j} - 2S_{\kappa_j}K_j^\top)\psi_j, \quad \kappa_j = k_j + i\sigma_j, \quad \sigma_j > 0, \\ \mathcal{A}_j &:= \frac{1}{2}I - 2S_{\kappa_j}N_j + S_{\kappa_j}Z_j - 2S_{\kappa_j}K_j^\top Z_j + K_j + S_j Z_j, \end{aligned} \quad (5.3)$$

where $Z_j = ik_0\varepsilon_j$. Thus the RtR operator \mathcal{S}^j can be expressed as

$$\mathcal{S}^j = I - 2Z_j\mathcal{A}_j^{-1}(S_j + S_{\kappa_j} - 2S_{\kappa_j}K_j^\top). \quad (5.4)$$

The generalized Robin conditions (4.5) and (4.11) are amenable to the same treatment provided in [33], the only difference being that the scalar impedance Z_j in equations (5.3) and (5.4) is replaced by impedance operators defined in equations (4.6) and (4.10) respectively.

Remark 5.1 *In the case of bounded subdomains Ω_j , the RtR operators \mathcal{S}_j can be computed robustly via the simpler formula*

$$\mathcal{S}_j = I - 2Z_j \left(\frac{1}{2}I + K_j + S_j Z_j \right)^{-1} S_j$$

which is more efficient in practice given that it entails fewer operator evaluations. In the case of the unbounded domain Ω_0 , the formula above cannot be shown to be robust for all frequencies k_0 , and thus the more complicated formula (5.4) is preferred. We also note that alternative robust BIE based calculations of interior/exterior RtR maps were provided in [31], yet those involve inversions of matrices twice as big as those require by equations (5.3) and (5.4) above.

In order to avoid complications related to singularities at junction/cross points, we replace in the DDM algorithm the RtR maps by *weighted* parametrized counterparts

$$\mathcal{S}^{j,w}(\varepsilon_j^{-1}|\mathbf{x}'_j|\partial_{n_j}u_j - i\eta u_j) := \varepsilon_j^{-1}|\mathbf{x}'_j|\partial_{n_j}u_j + i\eta u_j.$$

Collocated discretizations of the latter weighted RtR maps can be easily computed through a simple modification of the methodology introduced in [33] and recounted above. Nevertheless, the representation of RtR maps in terms of BIO requires use of inverses of the operators \mathcal{A}_j cf. equation (5.4). In order for the DDM algorithm to be efficient, the electric/acoustic size of subdomains Ω_j should be amenable to application of direct linear algebra solvers for calculations of the inverses of the collocation of the matrices \mathcal{A}_j . The discretization of the weighted RtR maps corresponding to each domain $\partial\Omega_j$ is thus constructed as $N_j \times N_j$ collocation matrices $\mathcal{S}_{N_j}^j$. Therefore, it is advisable to further subdivide the interior domains Ω_j when their size is deemed too large for efficient computations of their corresponding RtR maps. For the examples considered in this text, such subdivisions are straightforward as they consist of simply halving the subdomains.

In what follows we present a detailed algorithmic description of the DDM algorithms considered in this paper.

- 1 Offline: For each subdomain Ω_j , discretize all the BIO that feature in formula (5.3) corresponding to each boundary $\partial\Omega_j$ using Nyström discretizations. The discretization of each BIO in formula (5.3) results in a collocation matrix of size $N_j \times N_j$, whose computational cost is $\mathcal{O}(N_j^2)$;
- 2 Offline: Compute all the collocated subdomain RtR matrices $\mathcal{S}_{N_j}^j$ using formula (5.4) with $Z_j = ik_0\varepsilon_j$ and LU factorizations. Given that formula (5.4) matrix inverses, the cost of evaluating each subdomain RtR map is $\mathcal{O}(N_j^3)$;
- 3 Solution: Set up the DDM linear system according to formula (4.3) and solve for the Robin data f^N defined on the skeleton using GMRES;
- 4 Post-processing: Use the Robin data f^N computed in the previous step and the RtR matrices \mathcal{S}_N^j to compute Cauchy data on the boundary of each subdomain Ω_j .

Algorithm 1: Description of the DDM algorithm with classical Robin boundary conditions

- 1 Offline: For each subdomain Ω_j , discretize the operators $PS(\mathcal{T}_j)$ defined in formulas (4.10) using discrete Fourier transform matrices;
- 2 Offline: For each subdomain Ω_j , discretize all the BIO that feature in formula (5.3) corresponding to each boundary $\partial\Omega_j$ using Nyström discretizations. The discretization of each BIO in formula (5.3) results in a collocation matrix of size $N_j \times N_j$, whose computational cost is $\mathcal{O}(N_j^2)$;
- 3 Offline: Compute all the collocated subdomain Robin-to-Robin matrices \mathcal{S}_N^j using formula (5.4) with $Z_j = \varepsilon_j PS(\mathcal{T}_j)$ and LU factorizations. Given that formula (5.4) matrix inverses, the cost of evaluating each subdomain RtR map is $\mathcal{O}(N_j^3)$;
- 4 Solution: Set up the DDM linear system according to formula (4.3) and solve for the Robin data f^N defined on the skeleton using GMRES;
- 5 Post-processing: Use the Robin data f^N computed in the previous step and the RtR matrices \mathcal{S}_N^j to compute Cauchy data on the boundary of each subdomain Ω_j .

Algorithm 2: Description of the DDM GSQR algorithm.

- 1 Offline: For each subdomain Ω_j , compute collocated approximations of the complexified DtN operators $Y^{j,c}$ via equations (4.4). This step requires construction of collocation matrices for the discretization of complexified single and double layer operators, as well as inverses of the former. The computational cost of this stage is $\mathcal{O}(N_j^3)$;
- 2 Offline: Use the DtN matrices computed in the previous step and compute discretizations the operators \mathcal{T}_j^{DtN} defined in formulas (4.5). For a given subdomain, DtN matrices of adjacent subdomains are needed. The application of the projections in formula (4.5) simply amounts to extraction of suitable blocks from the DtN matrices;
- 3 Offline: For each subdomain Ω_j , discretize all the BIO that feature in formula (5.3) corresponding to each boundary $\partial\Omega_j$ using Nyström discretizations. The discretization of each BIO in formula (5.3) results in a collocation matrix of size $N_j \times N_j$, whose computational cost is $\mathcal{O}(N_j^2)$;
- 4 Offline: Compute all the collocated subdomain Robin-to-Robin matrices \mathcal{S}_N^j using formula (5.4) with $Z_j = \varepsilon_j \mathcal{T}_j^{DtN}$ and LU factorizations. Given that formula (5.4) matrix inverses, the cost of evaluating each subdomain RtR map is $\mathcal{O}(N_j^3)$;
- 5 Solution: Set up the DDM linear system according to formula (4.3) and solve for the Robin data f^N defined on the skeleton using GMRES;
- 6 Post-processing: Use the Robin data f^N computed in the previous step and the RtR matrices \mathcal{S}_N^j to compute Cauchy data on the boundary of each subdomain Ω_j .

Algorithm 3: Description of the DDM DtNR algorithm.

Schur complement solution of the DDM system described in Algorithm 1. In order to bypass the shortcomings of iterative solvers for DDM formulations (4.3), we resort to a direct solver of the same formulations that consists of application of hierarchical Schur complements without the need to manipulate the global DDM matrix. We begin by defining $L_{j\ell}$ be the subset of the set L_j corresponding to grid points that also belong to the interface $\Gamma_{j\ell}$. Accordingly, the collocated Robin data $f_j^{N_j}$ is split into interface Robin data so that $f_{j\ell}^{N_j}$ denotes the collocated Robin data at the grid points belonging to the set $L_{j\ell}$ defined above. For instance, in the case of three subdomains, we have that $f_1^{N_1} := [f_{10}^{N_1} \ f_{12}^{N_1}]^\top$, $f_2^{N_2} := [f_{20}^{N_2} \ f_{21}^{N_2}]^\top$, and $f_0^{N_0} := [f_{01}^{N_0} \ f_{02}^{N_0}]^\top$ respectively. This decomposition of Robin data into interface components gives rise to a splitting of the collocated RtR matrices $\mathcal{S}_{N_1}^1$ and $\mathcal{S}_{N_2}^2$ in the following block form

$$\mathcal{S}_{N_1}^1 = \begin{bmatrix} \mathcal{S}_{01,10}^1 & \mathcal{S}_{01,12}^1 \\ \mathcal{S}_{21,10}^1 & \mathcal{S}_{21,12}^1 \end{bmatrix} \quad \text{and} \quad \mathcal{S}_{N_2}^2 = \begin{bmatrix} \mathcal{S}_{02,20}^2 & \mathcal{S}_{02,21}^2 \\ \mathcal{S}_{12,20}^2 & \mathcal{S}_{12,21}^2 \end{bmatrix},$$

where the block matrix $\mathcal{S}_{01,10}^1$ denotes the submatrix block $\mathcal{S}_{N_1}^1(L_{10}, L_{10})$, and so forth. We similarly split the matrix $\mathcal{S}_{N_0}^0 = [\mathcal{S}_{10}^0 \ \mathcal{S}_{20}^0]$. These block decompositions/splittings of the Robin data and of the RtR matrices allows us to recast the DDM linear system described in Algorithm 1 into the following equivalent form

$$\begin{bmatrix} I & \mathcal{S}_{12,21}^2 & 0 & \mathcal{S}_{12,20}^2 & 0 \\ \mathcal{S}_{21,12}^1 & I & \mathcal{S}_{21,10}^1 & 0 & 0 \\ 0 & 0 & I & 0 & \mathcal{S}_{10}^0 \\ 0 & 0 & 0 & I & \mathcal{S}_{20}^0 \\ X_{01}\mathcal{S}_{01,12}^1 & X_{02}\mathcal{S}_{02,21}^2 & X_{01}\mathcal{S}_{01,10}^1 & X_{02}\mathcal{S}_{02,20}^2 & I \end{bmatrix} \begin{bmatrix} f_{12}^{N_1} \\ f_{21}^{N_2} \\ f_{10}^{N_1} \\ f_{20}^{N_2} \\ f_0^{N_0} \end{bmatrix} = \begin{bmatrix} 0 \\ 0 \\ (-\varepsilon_0^{-1} \partial_{n_0} u^{inc} + i\eta u^{inc})|_{L_{01}} \\ (-\varepsilon_0^{-1} \partial_{n_0} u^{inc} + i\eta u^{inc})|_{L_{02}} \\ (-\varepsilon_0^{-1} \partial_{n_0} u^{inc} - i\eta u^{inc})|_{L_0} \end{bmatrix}. \quad (5.5)$$

We note that the matrix in the new linear system (5.5) exhibits a block sparsity pattern that resembles that of matrices corresponding to two-dimensional finite difference operators that use five-point Laplaceans. We use a Schur complement approach for the solution of the linear system (5.5) that consists of elimination of the Robin data $(f_{12}^{N_1}, f_{21}^{N_2})$ corresponding to the interior interface Γ_{12} from the linear system (5.5). This procedure requires using the inverse of the matrix

$$\mathcal{D}_{12} := \begin{bmatrix} I & \mathcal{S}_{12,21}^2 \\ \mathcal{S}_{21,12}^1 & I \end{bmatrix}$$

which can be computed explicitly

$$\mathcal{D}_{12}^{-1} = \begin{bmatrix} I + \mathcal{S}_{12,21}^2 (I - \mathcal{S}_{21,12}^1 \mathcal{S}_{12,21}^2)^{-1} \mathcal{S}_{21,12}^1 & -\mathcal{S}_{12,21}^2 (I - \mathcal{S}_{21,12}^1 \mathcal{S}_{12,21}^2)^{-1} \\ -(I - \mathcal{S}_{21,12}^1 \mathcal{S}_{12,21}^2)^{-1} \mathcal{S}_{21,12}^1 & (I - \mathcal{S}_{21,12}^1 \mathcal{S}_{12,21}^2)^{-1} \end{bmatrix}. \quad (5.6)$$

We note that in order to compute the inverse matrix \mathcal{D}_{12}^{-1} we just need to invert the matrix $I - \mathcal{S}_{21,12}^1 \mathcal{S}_{12,21}^2$ whose size equals the number of grid points on the interface common to the subdomains Ω_1 and Ω_2 . Using the Schur complement \mathcal{D}_{12}^{-1} in equation (5.5) we obtain the following linear system

$$\begin{bmatrix} I & \mathcal{S}^0 \\ \mathcal{S}^{int} & I \end{bmatrix} \begin{bmatrix} f_0^{N_0, int} \\ f_0^{N_0} \end{bmatrix} = \begin{bmatrix} (-\varepsilon_0^{-1} \partial_{n_0} u^{inc} + i\eta u^{inc})|_{L_0} \\ (-\varepsilon_0^{-1} \partial_{n_0} u^{inc} - i\eta u^{inc})|_{L_0} \end{bmatrix}, \quad (5.7)$$

where $f_0^{N_0, int} = [f_{10}^{N_1} \ f_{20}^{N_2}]^\top$; we note that $f_0^{N_0, int}$ and $f_0^{N_0}$ have the same size N_0 . Interestingly, the matrix \mathcal{S}^{int} that features in equation (5.7) is itself a collocation matrix of the interior RtR whose definition is given by

$$\mathcal{S}^{int}(\psi) := (-\partial_{n_0} u - i\eta \varepsilon(x) u)|_{\partial\Omega_0}, \quad \varepsilon(x) = \varepsilon_1, \ x \in \Gamma_{10}, \ \varepsilon(x) = \varepsilon_2, \ x \in \Gamma_{20}, \quad (5.8)$$

where u is the solution of the following problem:

$$\begin{aligned} \Delta u + k(x)^2 u &= 0 \text{ in } \Omega_1 \cup \Omega_2, \quad k(x) = k_1, \ x \in \Omega_1, \ k(x) = k_2, \ x \in \Omega_2, \\ -\partial_{n_0} u + i\eta \varepsilon(x) u &= \psi \text{ on } \partial\Omega_0, \end{aligned}$$

and u and $\varepsilon(x)^{-1} \partial_n u$ are continuous across Γ_{12} where $\varepsilon(x) = \varepsilon_1, \ x \in \Omega_1, \ \varepsilon(x) = \varepsilon_2, \ x \in \Omega_2$, and $n = n_1 = -n_2$ on Γ_{12} . For obvious reasons, the procedure by which \mathcal{S}^{int} was obtained above can be interpreted as the merging of subdomain RtR matrices $\mathcal{S}_{N_j}^j, j = 1, 2$.

In the case of five subdomain configuration depicted in Figure 2, the Schur complement elimination procedure proceeds by rearranging the subdomain Robin data in the following order

$$f^N = [f_{12}^{N_1} \ f_{21}^{N_2} \ f_{34}^{N_3} \ f_{43}^{N_4} \ f_{23}^{N_2} \ f_{14}^{N_1} \ f_{32}^{N_3} \ f_{41}^{N_4} \ f_{10}^{N_1} \ f_{20}^{N_2} \ f_{30}^{N_3} \ f_{40}^{N_4} \ f_0^{N_0}]^\top$$

together with splittings of the RtR matrices $\mathcal{S}_{N_j}^j, j = 1, \dots, 4$ into 3×3 blocks and then (1) first eliminating the unknown pairs $[f_{12}^{N_1}, f_{21}^{N_2}]$ and $[f_{34}^{N_3}, f_{43}^{N_4}]$ in the first stage—this involves inversion of two matrices whose size equal to the number of grid points on the interfaces Γ_{12} and Γ_{34} , and (2) then subsequently eliminating the unknown pair $f_{top} := [f_{23}^{N_2}, f_{14}^{N_1}]$ and $f_{bottom} := [f_{32}^{N_3}, f_{41}^{N_4}]$ —this involves the inversion of a matrix whose size equal the number of grid points on $\Gamma_{14} \cup \Gamma_{23}$. After performing the Schur complement elimination stage we arrive at a sytem of the form (5.7) with $f_0^{N_0, int} = [f_{10}^{N_1} \ f_{20}^{N_2} \ f_{30}^{N_3} \ f_{40}^{N_4}]$ where the matrix \mathcal{S}^{int} represents a discretization of the RtR map in the domain $\Omega_1 \cup \Omega_2 \cup \Omega_3 \cup \Omega_4$ with piecewise continuous wavenumbers. Thus, the Schur elimination of

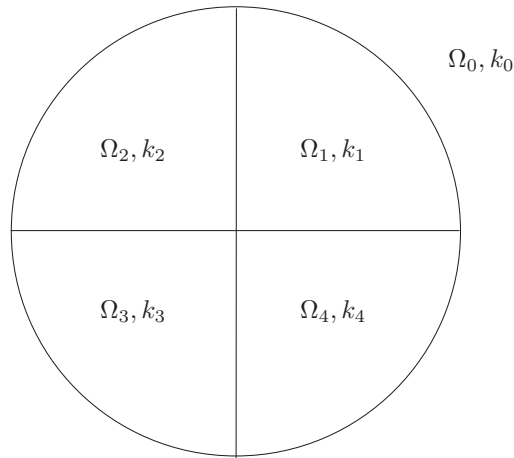


Figure 2: Five subdomain configuration.

the interior interface Robin data is equivalent to a hierarchical merging procedure of the subdomain RtR matrices [16] which can be efficiently applied to large numbers of subdomains. For this reason, this method of solution of the DDM linear system is referred to as Hierarchical Steklov-Poincaré solver [16].

The systems of the type (5.7) that result after the hierarchical merging of the RtR matrices corresponding to bounded subdomains, reduce in turn to the following equation involving the Robin unknowns $f_0^{N_0}$ defined on the interface $\partial\Omega_0$:

$$(I - \mathcal{S}^{int}\mathcal{S}^0)f_0^{N_0} = (-\varepsilon_0^{-1}\partial_{n_0}u^{inc} - i\eta u^{inc})|_{L_0} - \mathcal{S}^{int}(-\varepsilon_0^{-1}\partial_{n_0}u^{inc} + i\eta u^{inc})|_{L_0}. \quad (5.9)$$

Ideally, the linear system (5.9) should be solved by direct methods as well. Alternatively, if the size of the exterior Robin unknown $f_0^{N_0}$ becomes too large for application of direct linear algebra solvers, Krylov subspace iterative solvers such as GMRES [29] can be employed for the solution of the reduced system (5.9). We note that the matrix $I - \mathcal{S}^{int}\mathcal{S}^0$ is the collocated discretization of a pseudodifferential operator of order -1 (this can be rigorously established in the case when $k_1 = k_2$), and thus equation (5.9) does not possess ideal spectral properties for fast convergence of iterative Krylov subspace solvers. Alternative interior/exterior coupling strategies that possess superior spectral properties is subject of ongoing investigations.

- 1 Offline: relabel the bounded subdomains in a $P \times Q$ two dimensional array manner. A subdomain is denoted by Ω_{pq} where $1 \leq p \leq P$ denotes the row number, and $1 \leq q \leq Q$ denotes the column number of each subdomain;
- 2 Offline: For each subdomain Ω_{pq} , discretize all the BIO that feature in formula (5.3) corresponding to each boundary $\partial\Omega_{pq}$ using Nyström discretizations. The discretization of each BIO in formula (5.3) results in a collocation matrix of size $N_{pq} \times N_{pq}$, whose computational cost is $\mathcal{O}(N_{pq}^2)$;
- 3 Offline: Compute all the collocated subdomain Robin-to-Robin matrices \mathcal{S}_N^{pq} using formula (5.4) with $Z_{pq} = ik_0\varepsilon_{pq}$ and LU factorizations. Given that formula (5.4) matrix inverses, the cost of evaluating each subdomain RtR map is $\mathcal{O}(N_{pq}^3)$;
- 4 Block splitting of RtR matrices: Split each RtR matrix into blocks corresponding to adjacent subdomains.;
- 5 Horizontal sweep: for each $p = 1, \dots, P$, perform the merging of RtR matrices $\mathcal{S}_{N_{pq}}^{pq}, q = 1, \dots, Q$ corresponding to adjacent row subdomains. When a merging is performed, inverses of matrices that feature in equation (5.6) need be computed by LU factorizations. The size of the matrices that need be inverted equals to the number of grid points on the common interfaces of the merged subdomains. We obtain as a result, merged $\mathcal{S}_p, p = 1, \dots, P$ RtR matrices corresponding to the union of all subdomains corresponding to the same row in the domain decomposition;
- 6 Vertical sweep: Perform the vertical merging of the matrices \mathcal{S}_p produced in the previous step. Again, inverses of the same type of matrices are needed. We obtain as a results a RtR matrix corresponding to the union of all bounded domains;
- 7 Solution: Solve equation (5.9) using either LU factorizations or GMRES;
- 8 Post-processing: Use the Robin data $f_0^{N_0}$ computed in the previous step and the RtR matrices \mathcal{S}_N^j to compute Cauchy data on the boundary of each subdomain Ω_j .

Algorithm 4: Description of the hierarchical Schur complement DDM algorithm.

Alternatively, the merging of the RtR maps described in Algorithm 4 can be performed hierarchically via an octree arrangement of the subdomains.

6 Numerical results

In this section we present numerical experiments with for each one of the various formulations of the transmission problems (2.1) considered in this text. We use, as test configurations with piece-wise constant dielectric permittivities ε_j , the circular structures depicted in Figures 1 and 2, in which the circular domain has radius one. All of the formulations considered were discretized following the prescription in Section 5. We used discretizations that place the same number of discretization points on each interface—matching boundary meshes, and sigmoid transforms of polynomial degree 3 for the MTF equation (3.12) and the DDM formulation (4.3) with $\eta = k_0$, and respectively degree 4 for the STF (3.17). We select $\sigma_j = 0.1$ in the definition of the operators (4.5) incorporated in the DDM DtNR and, respectively, $\sigma_j = k_j^{1/3}$ in the definition of the operators (4.10) that are incorporated in DDM GSqR. In all the numerical experiments we present numbers of GMRES iterations for various solvers to reach a relative residual of 10^{-4} and present errors in the far-field for 1024 equi-spaced far-field directions. The far-field errors were computed using fine

DDM (5.5)		DDM Schur (5.9)		4 DDM (5.5)		4 DDM Schur (5.9)		MTF				STF (3.17)	
It	ε_∞	It		It	ε_∞	It		It (3.12)	It (3.13)	It (3.15)	ε_∞	It	ε_∞
77	4.1×10^{-3}	22		107	4.5×10^{-3}	23		142	102	77	3.6×10^{-3}	67	1.4×10^{-3}
73	3.4×10^{-4}	22		118	3.5×10^{-4}	22		145	104	78	2.8×10^{-4}	69	1.7×10^{-4}

Table 1: Far-field errors computed using various formulations considered in this text in the three subdomain case with $\varepsilon_0 = 1$, $\varepsilon_1 = 4$, $\varepsilon_2 = 16$ and $\omega = 2$. The numbers of unknowns required by the DDM and STF are 192 and 384 respectively; the MTF uses twice as many unknowns in each case. We present results for the DDM formulations in the case when the subdomains Ω_1 and Ω_2 are each subdivided into two subdomains, and we refer to these cases by 4 DDM.

ω	DDM (5.5)				DDM Schur (5.9)		MTF				STF (3.17)	
	It	It DtNR	It GSqR	ε_∞	It	ε_∞	It (3.12)	It (3.13)	It (3.15)	ε_∞	It	ε_∞
1	137	16	25	4.8×10^{-3}	15	4.9×10^{-3}	431	242	160	5.3×10^{-3}	159	3.9×10^{-3}
2	182	19	40	1.8×10^{-3}	18	2.6×10^{-3}	750	433	293	2.4×10^{-3}	270	3.2×10^{-3}
4	282	19	68	2.9×10^{-3}	20	1.3×10^{-3}	1,335	732	508	3.4×10^{-3}	430	2.8×10^{-3}
8	518	18	100	2.4×10^{-3}	33	1.8×10^{-3}	2,555	1,431	1,001	2.7×10^{-3}	800	2.6×10^{-3}

Table 2: Performance of the various formulations considered in this text in the three subdomain case with $\varepsilon_0 = 1$, $\varepsilon_1 = 64$, and $\varepsilon_2 = 256$. The numbers of unknowns required by the DDM and STF are 384, 768, 1536, and 3072 respectively; the MTF uses twice as many unknowns in each case.

discretizations of the MTF solver. As previously mentioned, the discretizations of both STF and the DDM formulations use the same number of unknowns, whereas that of MTF uses twice as many unknowns.

We start the presentation of numerical results with an illustration in Table 1 of the accuracy of our solvers based on the MTF, STF, and various DDM algorithms considered in this text. In all the numerical results presented, the accuracy achieved by the DDM GSqR and DDM DtN solvers is at the same level to that of the DDM solver in all of the cases considered, and for this reason and in order to better streamline the information presented we chose not to report it. We continue in Tables 2 and 3 with an illustration of the performance of the three types of solvers discussed in this text in the case of multiple junction configurations with very high-contrast materials for various frequencies ω . We report in Figure 3 the numbers of GMRES iterations required by the various formulations for two cases of piece-wise composite dielectrics in the high-frequency regime; in that figure we denoted by the MTF the preconditioned MTF (3.15) that performs best among the three MTF versions considered in this text. In addition, we depict in Figure 4 a simulation of the fields inside and near various dielectric composite structures under plane wave excitations.

ω	DDM (5.5)				DDM Schur (5.9)		MTF				STF (3.17)	
	It	It DtNR	It GSqR	ε_∞	It	ε_∞	It (3.12)	It (3.13)	It (3.15)	ε_∞	It	ε_∞
1	977	39	70	1.6×10^{-3}	12	1.9×10^{-3}	2,419	1,296	1,107	4.5×10^{-3}	942	1.1×10^{-3}
2	1,788	72	140	2.9×10^{-3}	20	3.3×10^{-3}	4,534	2,442	2,154	5.4×10^{-3}	1,782	2.1×10^{-3}
4	2,503	123	278	1.0×10^{-3}	22	1.3×10^{-3}	6,695	3,486	3,073	5.1×10^{-3}	3,243	6.9×10^{-4}

Table 3: Performance of the various formulations considered in this text in the five subdomain case with $\varepsilon_0 = 1$, $\varepsilon_1 = 64$, $\varepsilon_2 = 256$, $\varepsilon_3 = 1024$, and $\varepsilon_4 = 4096$. The numbers of unknowns required by the DDM and STF are 4608, 9216, and 15360 respectively; the MTF uses twice as many unknowns in each case.

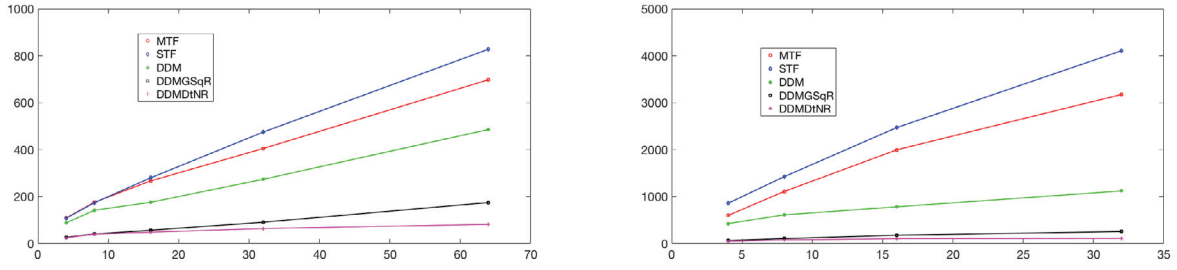


Figure 3: Numbers of iterations required by the various formulations considered in this text in the three subdomain case with $\varepsilon_0 = 1$, $\varepsilon_1 = 4$, and $\varepsilon_2 = 16$ and frequencies $\omega = 4, 8, 16, 32, 64$ (left). Numbers of iterations required by the various formulations considered in this text in the five subdomain case with $\varepsilon_0 = 1$, $\varepsilon_1 = 4$, $\varepsilon_2 = 16$, $\varepsilon_3 = 64$, and $\varepsilon_4 = 256$ and frequencies $\omega = 4, 8, 16, 32$ (right).

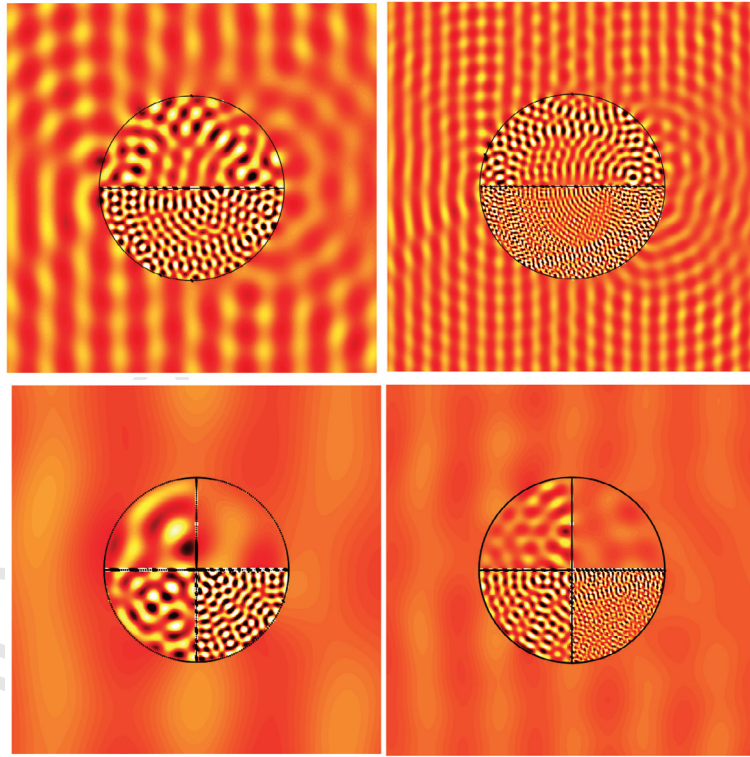


Figure 4: Plots of the near fields scattered by multiple junction configurations under plane wave incidence of direction $d = (1, 0)$. Top panel: $\varepsilon_0 = 1$, $\varepsilon_1 = 4$, and $\varepsilon_2 = 16$; $\omega = 16$ (left) and $\omega = 32$ (right). Bottom panel: $\varepsilon_0 = 1$, $\varepsilon_1 = 4$, $\varepsilon_2 = 16$, $\varepsilon_3 = 64$, and $\varepsilon_4 = 256$; $\omega = 4$ (left) and $\omega = 8$ (right)

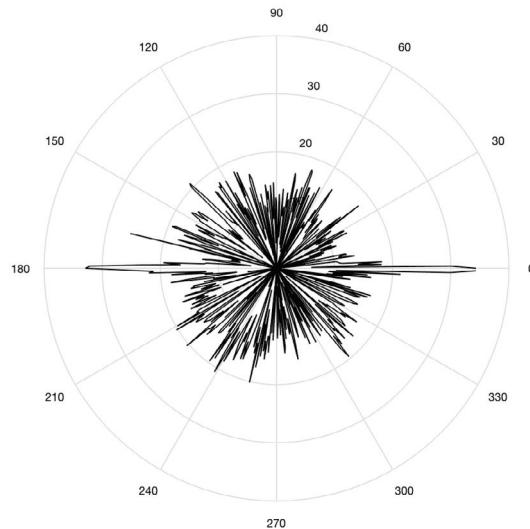


Figure 5: RCS plot of the far-field scattered by a checkerboard structure comprised of a 16×16 array of squares of size 4 such that the electric permittivity in each square is a random number in the interval $[2, 256]$, $\varepsilon_0 = 1$ and $\omega = 4$. The scattered field was computed via the Schur complement solution of the DDM system using 278528 unknowns on the skeleton of the composite structure.

Discussion of the performance of various formulations. We begin by noting that the computational cost of setting up the MTF equation (3.12) and the STF (3.17) is comparable, as the building blocks of these formulations are the same BIO defined on the boundaries of the subdomains. The behavior of iterative solvers for the solution of Nyström discretizations of the two formulations is quite different, given that MTF is a first kind formulation that requires twice as many unknowns than the second kind formulation STF. Calderón preconditioning strategies that lead to the MTF formulation (3.13) and Schur complement strategies combined with Calderón preconditioning strategies that lead to the MTF formulation (3.15) are effective in reducing the numbers of GMRES iterations and do not require significant additional computational costs. In contrast, the STF (3.17), whose motivation was canceling the adverse effects of hypersingular operators, is not easily amenable to analytic preconditioning. However, even with MTF preconditioning, both formulations require large numbers of GMRES iterations, especially in the case of high-contrast multi-domain configurations at high-frequencies.

As it can be seen from the results presented in this section, solvers based on DDM formulations (4.3) and the DDM formulation that incorporate either the DtNR or GSqR transmission conditions give rise to smaller numbers of GMRES iterations than those based on the MTF and STF. We note that effecting the matrix-vector product associated with the DDM equation (4.3), requires in turn application of each of the RtR maps \mathcal{S}^j . The latter require solutions of Robin/impedance boundary value problems in each corresponding domain Ω_j via equations (5.3), which can be performed either iteratively or using LU factorizations. If iterative solvers are employed for the application of RtR maps, the numbers of iterations grow quickly with the frequency for bounded/interior subdomains [33]. For this reason we used LU factorization for the application of RtR maps. As described in Section 5, the DDM algorithms proceed in two stages: (1) a precomputation/offline stage where

ω	DDM (5.5)			4 DDM (5.5)			
	It	It DtNR	It GSqR	It	It DtNR	It GSqR	
1	137	16	25	225	42	44	
2	182	19	40	361	61	73	
4	282	19	68	597	104	129	
4	88	31	30	153	46	37	
8	142	40	54	231	64	63	
16	176	49	77	257	78	78	
32	274	64	106	367	101	130	

Table 4: Left panel: numbers of GMRES iterations needed to reach a residual of 10^{-4} for the solution of equation (5.3) in each subdomain and respectively for the solution of the global DDM system (4.3) in the three subdomain case with $\varepsilon_0 = 1$, $\varepsilon_1 = 64$, and $\varepsilon_2 = 256$ (top three rows) and $\varepsilon_0 = 1$, $\varepsilon_1 = 4$, and $\varepsilon_2 = 16$ (bottom four rows). Right panel: same numbers of GMRES iterations when the subdomains Ω_1 and Ω_2 are each subdivided into two half-sized non-overlapping subdomains $\Omega_1 = \Omega_{11} \cup \Omega_{12}$ and $\Omega_2 = \Omega_{21} \cup \Omega_{22}$ respectively.

all the subdomain RtR maps are precomputed, and (2) an online stage where the DDM linear system is solved iteratively in a matrix-free fashion. We note that the use of GSqR transmission conditions (4.10) in the DDM algorithm gives rise to important savings in numbers of iterations with virtually no additional cost with respect to the DDM with classical Robin transmission conditions. The numbers of iterations required by DDM algorithm with DtNR transmission conditions if further decreased, yet at the expense of adding one more offline stage (0) in which the subdomain DtN maps are precomputed. We mention that the use of Nyström discretizations allows for a relatively seamless incorporation of both GSqR and DtNR transmission conditions in the DDM framework. The square root operators that enter the GSqR transmission conditions (4.10) can be replaced by suitable Padé approximations that allow for their incorporation in a Galerkin/boundary element DDM framework [4]. The use of DtNR transmission conditions becomes more problematic in three dimensions due to the significant additional computational cost required for the evaluation of DtN maps.

In the light on the discussion above on the role that the size of the subdomains plays in the efficient computation of the RtR maps, we investigate in Table 4 the influence of the number of subdomains and their adjacency graph on the iterative behavior of the DDM with various transmission conditions. Clearly, the number of subdomains and their electrical size and adjacency graph adversely affects the rate of convergence of iterative solvers of the DDM system (4.3), regardless of the type of transmission boundary conditions used. As it can be seen from the results in Table 4, the numbers of iterations required by the DDM considered in this text grow proportionally with the frequency and number of subdomains. An explanation of this fact is that although the GSqR and DtNR transmission conditions optimize the local data exchange between adjacent subdomains, the DDM iterations still have to resolve the global exchange of data between all subdomains. The latter exchange can be accelerated by the use of double sweep preconditioners in DDM with slab-type subdomain decompositions (i.e. the adjacency graph is a tree). Indeed, it was shown in [34] that the use of double sweep preconditioners in conjunction with optimized transmission conditions give rise to DDM that scale with the frequency and the number of subdomains in the absence of sharp interface of material discontinuity. The incorporation of double sweep preconditioners for various transmission condition DDM is currently underway.

Finally, the Schur complement solution of the DDM system can be viewed as a computational alternative to iterative DDM solvers in the case of large numbers of subdomains that require large-

sized skeleton discretizations. Indeed, if equation (5.9) is solved either via direct linear algebra solvers, then the hierarchical Schur complement approach is a direct solver of the DDM linear system whose cost is $\mathcal{O}(N^{3/2})$ where N is the number of unknowns used to discretize the Robin data defined on the two-dimensional skeleton. We present in Figure 5 a simulation of the Radar Cross Section (RCS) of the far-field scattered by a checkerboard structure comprised of a 16×16 array of squares of size 4 whose electric permittivities are chosen randomly in the interval $[2, 256]$, the electric permittivity of the unbounded domain is $\varepsilon_0 = 1$ and $\omega = 4$. We used 278,528 unknowns on the skeleton of the composite structure to discretize the DDM linear system whose solution was performed via the hierarchical Schur complement algorithm; the solution time was 124 seconds on a MacBookPro machine with 2×2.3 GHz Quad-core Intel i7 with 16 GB of memory. Once the RtR maps of interior domains have been hierarchically merged to produce the RtR map \mathcal{S}^{int} , the equation (5.9) can be also solved iteratively. As it can be seen from the results presented in this section, the number of GMRES iterations needed to solve equation (5.9) is quite reasonable throughout the range of problems considered, and does not appear to grow dramatically with the frequency. Nevertheless, equation (5.9) shares the same features with integral equations of the first kind, alternative robust interior/exterior coupling strategies are desirable. One possibility currently under investigation is to use GSqR transmission conditions (4.10). However, a potential drawback of the Schur complement solution of the DDM linear system is its $\mathcal{O}(N^2)$ computational cost in three dimensions.

7 Conclusions

We presented a comparison between the performance of Krylov subspace iterative solvers based on Nyström discretizations of Multiple Trace Formulations (MTF), Single Trace Formulations (STF), and Domain Decomposition Methods (DDM) for two dimensional frequency domain scattering problems involving bounded composite materials, i.e. piece-wise constant material parameters. We investigated DDM based on both classical Robin transmission conditions as well as optimized transmission boundary conditions. The former DDM version gives rise to linear systems which, although not particularly well-suited for iterative solvers, can be solved efficiently via Schur complements. On the other hand, the DDM versions with optimized transmission conditions that incorporates square root approximations of DtN maps gives rise to relatively small numbers of iterations. Extensions to three-dimensional configurations are currently underway.

Acknowledgments

Catalin Turc gratefully acknowledges support from NSF through contracts DMS-1312169 and DMS-1614270. Carlos Jerez-Hanckes thanks partial support from Conicyt Anillo ACT1417.

References

- [1] X. Antoine and M. Darbas. Alternative integral equations for the iterative solution of acoustic scattering problems. *Quart. J. Mech. Appl. Math.*, 58(1):107–128, 2005.

- [2] X. Antoine and M. Darbas. Generalized combined field integral equations for the iterative solution of the three-dimensional Helmholtz equation. *M2AN Math. Model. Numer. Anal.*, 41(1):147–167, 2007.
- [3] Alvin Bayliss, Charles I Goldstein, and Eli Turkel. An iterative method for the helmholtz equation. *Journal of Computational Physics*, 49(3):443–457, 1983.
- [4] Y. Boubendir, X. Antoine, and C. Geuzaine. A quasi-optimal non-overlapping domain decomposition algorithm for the Helmholtz equation. *J. Comput. Phys.*, 231(2):262–280, 2012.
- [5] Y. Boubendir, O. Bruno, C. Levadoux, and C. Turc. Integral equations requiring small numbers of Krylov-subspace iterations for two-dimensional smooth penetrable scattering problems. *Appl. Numer. Math.*, 95:82–98, 2015.
- [6] Y. Boubendir and C. Turc. Wave-number estimates for regularized combined field boundary integral operators in acoustic scattering problems with neumann boundary conditions. *IMA Journal of Numerical Analysis*, 33(4):1176–1225, 2013.
- [7] Yassine Boubendir and Catalin Turc. Well-conditioned boundary integral equation formulations for the solution of high-frequency electromagnetic scattering problems. *Computers & Mathematics with Applications*, 67(10):1772–1805, 2014.
- [8] X. Claeys, R. Hiptmair, and C. Jerez-Hanckes. Multitrace boundary integral equations. In *Direct and inverse problems in wave propagation and applications*, volume 14 of *Radon Ser. Comput. Appl. Math.*, pages 51–100. De Gruyter, Berlin, 2013.
- [9] Xavier Claeys, Ralf Hiptmair, and Elke Spindler. A second-kind galerkin boundary element method for scattering at composite objects. *BIT Numerical Mathematics*, 55(1):33–57, 2015.
- [10] D. Colton and R. Kress. *Integral equation methods in scattering theory*. Pure and Applied Mathematics (New York). John Wiley & Sons Inc., New York, 1983. A Wiley-Interscience Publication.
- [11] Bruno Després. Décomposition de domaine et problème de Helmholtz. *C. R. Acad. Sci. Paris Sér. I Math.*, 311(6):313–316, 1990.
- [12] Björn Engquist and Lexing Ying. Sweeping preconditioner for the helmholtz equation: hierarchical matrix representation. *Communications on pure and applied mathematics*, 64(5):697–735, 2011.
- [13] Yogi A Erlangga, Cornelis Vuik, and Cornelis Willebrordus Oosterlee. On a class of preconditioners for solving the helmholtz equation. *Applied Numerical Mathematics*, 50(3):409–425, 2004.
- [14] Martin J. Gander, Frédéric Magoulès, and Frédéric Nataf. Optimized Schwarz methods without overlap for the Helmholtz equation. *SIAM J. Sci. Comput.*, 24(1):38–60 (electronic), 2002.
- [15] S. Ghanemi, F. Collino, and P. Joly. Domain decomposition method for harmonic wave equations. In *Mathematical and numerical aspects of wave propagation (Mandelieu-La Napoule, 1995)*, pages 663–672. SIAM, Philadelphia, PA, 1995.

- [16] Adrianna Gillman, Alex H. Barnett, and Per-Gunnar Martinsson. A spectrally accurate direct solution technique for frequency-domain scattering problems with variable media. *BIT*, 55(1):141–170, 2015.
- [17] L Greengard, Kenneth L. Ho, and J.-Y. Lee. A fast direct solver for scattering from periodic structures with multiple material interfaces in two dimensions. *J. Comput. Phys.*, 258:738–751, 2014.
- [18] R. Hiptmair and C. Jerez-Hanckes. Multiple traces boundary integral formulation for Helmholtz transmission problems. *Adv. Comput. Math.*, 37(1):39–91, 2012.
- [19] R. Hiptmair, C. Jerez-Hanckes, J.-F. Lee, and Z. Peng. Domain decomposition for boundary integral equations via local multi-trace formulations. In J. Erhel, M.J. Gander, L. Halpern, G. Pichot, T. Sassi, and O. Widlund, editors, *Domain Decomposition Methods in Science and Engineering XXI*, volume 98 of *Lecture Notes in Computational Science and Engineering*, pages 43–58, Berlin, 2014. Springer.
- [20] Carlos Jerez-Hanckes, José Pinto, and Simon Tournier. Local multiple traces formulation for high-frequency scattering problems. *Journal of Computational and Applied Mathematics*, 289:306–321, 2015.
- [21] Carlos Jerez-Hanckes, José Pinto, and Simon Tournier. Scientific computing in electrical engineering. In Andreas Bartel, Markus Clemens, Michael Günther, and E. Jan W. ter Maten, editors, *Local Multiple Traces Formulation for High-Frequency Scattering Problems by Spectral Elements*, number 23 in *Mathematics in Industry*. Springer International Publishing Switzerland, 2016.
- [22] R. Kress. A Nyström method for boundary integral equations in domains with corners. *Numer. Math.*, 58(2):145–161, 1990.
- [23] R. Kussmaul. Ein numerisches Verfahren zur Lösung des Neumannschen Aussenraumproblems für die Helmholtzsche Schwingungsgleichung. *Computing (Arch. Elektron. Rechnen)*, 4:246–273, 1969.
- [24] E. Martensen. Über eine Methode zum räumlichen Neumannschen Problem mit einer Anwendung für torusartige Berandungen. *Acta Math.*, 109:75–135, 1963.
- [25] W. McLean. *Strongly elliptic systems and boundary integral equations*. Cambridge University Press, Cambridge, 2000.
- [26] C. Müller. *Foundations of the mathematical theory of electromagnetic waves*. Revised and enlarged translation from the German. Die Grundlehren der mathematischen Wissenschaften, Band 155. Springer-Verlag, New York, 1969.
- [27] Frédéric Nataf. Interface connections in domain decomposition methods. In *Modern methods in scientific computing and applications (Montréal, QC, 2001)*, volume 75 of *NATO Sci. Ser. II Math. Phys. Chem.*, pages 323–364. Kluwer Acad. Publ., Dordrecht, 2002.
- [28] Michael Pedneault, Catalin Turc, and Yassine Boubendir. Schur complement domain decomposition methods for the solution of multiple scattering problems. *arXiv preprint arXiv:1608.00034*, 2016.

- [29] Y. Saad and M.H. Schultz. GMRES: a generalized minimal residual algorithm for solving nonsymmetric linear systems. *SIAM J. Sci. Statist. Comput.*, 7(3):856–869, 1986.
- [30] Elke Spindler. *Second kind single-trace boundary integral formulations for scattering at composite objects*. PhD thesis, 2016.
- [31] O Steinbach and M Windisch. Stable boundary element domain decomposition methods for the helmholtz equation. *Numerische Mathematik*, 118(1):171–195, 2011.
- [32] Christiaan C Stolk. A rapidly converging domain decomposition method for the helmholtz equation. *Journal of Computational Physics*, 241:240–252, 2013.
- [33] Catalin Turc, Yassine Boubendir, and Mohamed Kamel Riahi. Well-conditioned boundary integral equation formulations and nyström discretizations for the solution of helmholtz problems with impedance boundary conditions in two-dimensional lipschitz domains. *arXiv preprint arXiv:1607.00769*, 2016.
- [34] Alexandre Vion and Christophe Geuzaine. Double sweep preconditioner for optimized schwarz methods applied to the helmholtz problem. *Journal of Computational Physics*, 266:171–190, 2014.
- [35] Leonardo Zepeda-Núñez and Laurent Demanet. The method of polarized traces for the 2d helmholtz equation. *Journal of Computational Physics*, 308:347–388, 2016.